Br. J. Pharmac. (1986), **88**, 291–297

Pharmacological analysis of the inhibition by pirenzepine and atropine of vagal-stimulated acid secretion in the isolated stomach of the mouse

J.W. Black & N.P. Shankley

The Rayne Institute, King's College Hospital Medical School, Denmark Hill, London SE5 8RX

1 The muscarinic receptors involved in the vagal stimulation of gastric acid secretion in the mouse isolated stomach assay have been examined by analysing the effects of pirenzepine and atropine on fully-defined frequency-effect curves.

2 Both atropine and pirenzepine produced concentration-dependent inhibition of vagal-stimulated acid secretion in a manner consistent with a model describing competitive antagonism of endogenous acetylcholine, which was assumed to be released by vagal stimulation.

3 The results obtained are quite compatible with the hypothesis that vagal stimulation involves muscarinic receptors which are homogeneous with those previously found on histamine and oxyntic cells in the mouse stomach assay.

4 These results find no evidence for muscarinic receptor heterogeneity and reinforce the hypothesis that the selectivity of pirenzepine *in vivo* relative to atropine is due to the loss of atropine into the gastric secretion.

Introduction

Angus & Black (1982) first reported that electrical field stimulation of acid secretion by the isolated, lumen-perfused, stomach preparation of the mouse was abolished with either tetrodotoxin or atropine; therefore they concluded that the stimulation was mediated by vagal nerve endings. The concentrations of atropine needed to inhibit this secretion were similar to those previously found necessary to antagonize competitively acid secretion produced by the choline esters carbachol or bethanechol in the same assay (Angus & Black, 1979). Apparently, atropine did not discriminate between muscarinic receptors presumed to be involved in vagal stimulation and those stimulated by the choline esters.

Since then, Pagani *et al.* (1984) and Schiavone *et al.* (1985), using pirenzepine, classified as a selective, muscarinic M_1-receptor antagonist, concluded that the muscarinic receptors involved in the vagal stimulation of acid secretion in the isolated stomach of the mouse were of the M_1-subtype in contrast to those of the M_2-subtype, presumed to be present on the oxyntic cell and stimulated by choline esters. This conclusion was based on the ratios of concentrations of atropine and pirenzepine needed to inhibit by 50% (IC_{50}) a single response to both bethanechol and vagal-stimulated acid secretion. In this study, we extend their analysis by examining the effects of pirenzepine and atropine on fully-defined frequency-effect curves on an improved, isolated stomach assay preparation of the mouse (Black & Shankley, 1985a).

An abstract of this work has previously been presented to the Second International Symposium on 'Subtypes of Muscarinic Receptors' (Black & Shankley, 1985d).

Methods

Acid secretion

Gastric acid secretion was measured in the isolated, lumen-perfused, stomach preparation of the mouse as described previously (Black & Shankley, 1985a). Briefly, stomach preparations were established with the pH-electrode system arranged to provide a 12 cm H_2O pressure to distend the stomach. Six preparations were used simultaneously and, after an initial 60 min period, those not producing a stable basal acid secretion (approximately 5%) were rejected. All drugs were added directly to the organ bath (serosal side) and, following a further 60 min equilibration period in the absence or presence of antagonist, a single

cumulative agonist concentration-effect or frequency-effect curve was obtained. Physostigmine, 10^{-7} M, administered at 60 min, was present throughout the experiments to inhibit acetylcholinesterase.

Field stimulation

Electrical field stimulation of the vagus was achieved, essentially, by the methods used by Angus & Black (1982). A pair of platinum, ring, electrodes (ring diameter 2 mm, wire diameter 0.5 mm) were placed either side of the stomach to stimulate the region of the fundic glands. The intensity of stimulation was standardized at 10 V with square wave pulses of 0.5 ms duration. Single, cumulative, frequency-effect curves were obtained over a frequency range of 1 to 30 Hz. Stimulation at frequencies above 30 Hz invariably caused visible tissue damage and rupturing of the stomachs.

Experimental design

Antagonist treatments were allocated on a block design such that, as far as possible, all organ baths received each treatment during the course of an experiment.

Analysis

Acid secretion responses produced by acetylcholine and vagal stimulation were measured as the change in pH (ΔpH) of the lumen perfusate referred to that immediately prior to starting the cumulative concentration-effect or frequency-effect curves. Curve data from individual preparations were fitted, by an iterative least squares computer programme (locally written), to a logistic function of the form.

$$E = \frac{a[A]^n}{[A_{50}]^n + [A]^n},$$

in which E is effect and a, $[A_{50}]$ and n are the maximal asymptote, midpoint location and slope parameters

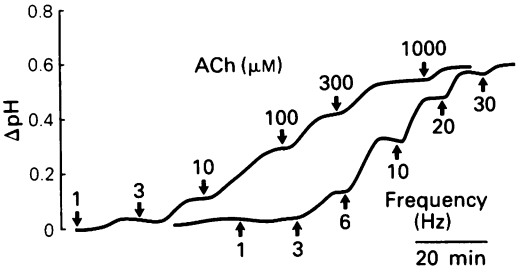

Figure 1 Cumulative concentration-effect and frequency-effect curves, in the mouse isolated stomach, to acetylcholine (ACh) and electrical field stimulation in the presence of 10^{-7} M physostigmine. In this and subsequent figures Δ pH (ordinate scale) refers to the change in pH of the lumen perfusate (1 ml min^{-1}). The concentrations of acetylcholine and frequency of stimulation were increased upon attainment of a steady-state response.

respectively. The parameters a, $\log[A_{50}]$ and n are assumed to be distributed normally and are presented as means ± s.e. For graphical purposes the individual computed parameter estimates for each treatment group were expressed as means and a single logistic curve was generated and superimposed upon the combined experimental data for display on a log scale in the usual way.

Model fitting

A BMDP Module AR (Dixon, 1981) computer programme was used to perform derivative-free, non-linear, regression of experimental data to the models detailed in the theoretical section.

Drugs

Drugs were prepared freshly in distilled water. The total volume added to the 40 ml organ bath did not exceed 800 μl. Drugs and their sources were as follows: atropine sulphate (Sigma), physostigmine (Sigma),

Table 1 Acetylcholine-effect and frequency-effect logistic curve fitting parameters

	No. of replicates	*Midpoint location parameter*	*Maximal asymptote (a)* (ΔpH)	*Slope* (n)
Acetylcholine	6	−4.94 ± 0.14†	0.65 ± 0.03	0.90 ± 0.05
Frequency	6	0.85 ± 0.02‡	0.58 ± 0.05	2.28 ± 0.29*

*Significantly different from unity.
†Log $[A_{50}]$.
‡Log (frequency) required for 0.5 a.

acetylcholine iodide (BDH Chemicals Ltd), pirenzepine dihydrochloride (a generous gift from A.B. Hassle Ltd).

Results

Frequency-effect and acetylcholine concentration-effect curves

Electrical field stimulation produced frequency-dependent, and acetylcholine produced concentration-dependent, sustained increases in basal gastric acid secretion (Figure 1). The electrically-stimulated responses were totally abolished by pretreatment with 10^{-7} M tetrodotoxin (data not shown) in agreement with the previous results of Angus & Black (1982).

Logistic curve fitting of the individual experimental data gave the mean parameter estimates presented in Table 1. These parameters were used to simulate the logistic curves shown superimposed upon experimental data in Figure 2.

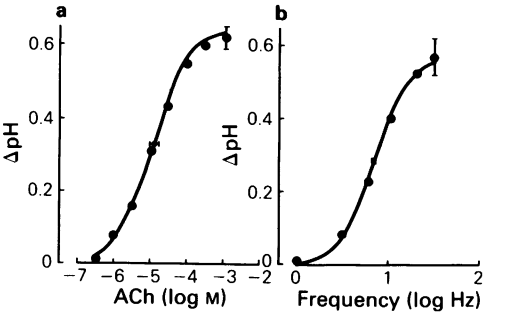

Figure 2 Logistic concentration-effect (a) and frequency-effect (b) curves to acetylcholine (ACh) and electrical field stimulation of the vagus in the mouse stomach. The best-fit logistic curves are superimposed upon the mean experimental data points ($n = 6 \pm$ s.e. The horizontal bars represent the standard errors of the best-fit values of A_{50} or f_{50}.

Frequency-effect curves in the presence of atropine and pirenzepine

Both atropine and pirenzepine produced concentration-dependent rightward displacement and depression of the maximal asymptote of the frequency-effect curves (Figure 3). These effects of the muscarinic antagonists were seen at concentrations within the range which was previously found to antagonize competitively the effects of 5-methylfurmethide (Black & Shankley, 1985b) and McN-A343 (Black & Shankley, 1985c) in the mouse stomach.

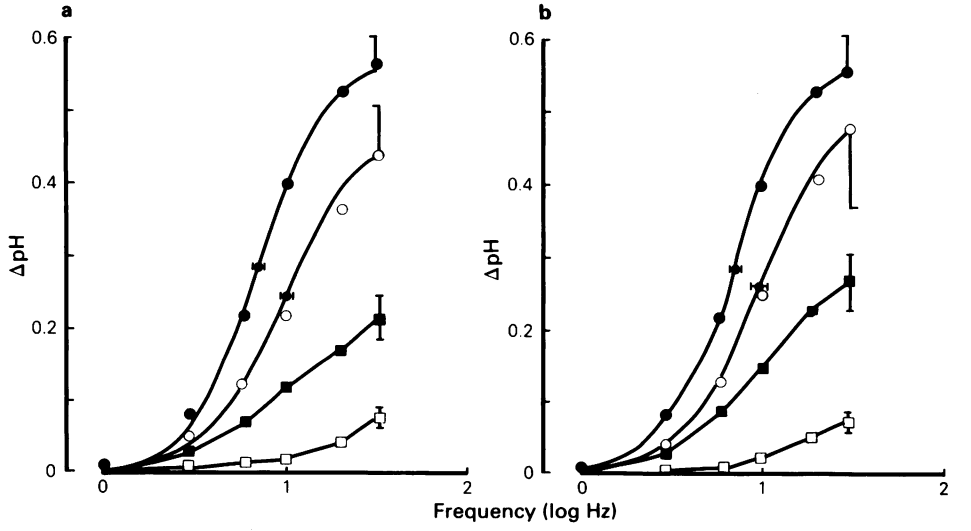

Figure 3 (a) The effects of atropine (●) 0.0, (○) 3×10^{-8}, (■) 3×10^{-7}, (□) 3×10^{-6} M, on frequency-effect curves obtained in the presence of 10^{-7} M physostigmine. (b) The effect of pirenzepine (●) 0.0, (○) 3×10^{-7}, (■) 10^{-6}, (□) 10^{-5} M, on frequency-effect curves obtained in the presence of 10^{-7} M physostigmine. Due to the almost maximal inhibition of some of the frequency-effect curves in the presence of atropine (3×10^{-7}, 3×10^{-6} M) and pirenzepine (10^{-6}, 10^{-5} M) it was not possible to fit individual logistic curves to these data. Mean experimental data points (n = 4/6) are shown with vertical lines representing s.e.

A model describing the competitive antagonism of acetylcholine released by the vagus during electrical stimulation

In a previous study (Black *et al.*, 1985), a model of indirect agonism was developed describing the acid secretory activity of pentagastrin and its inhibition by the histamine H_2-receptor antagonist, tiotidine. The same analytical approach is used here and begins by characterizing the frequency-effect function and then proceeds by identifying an input function and a transducer function which originally produced that output function. Thus, electrical stimulation (frequency) is assumed to release acetylcholine which, in turn, stimulates gastric acid secretion. The problem is to identify the nature of the frequency-acetylcholine and acetylcholine-effect functions which, in sequence, provide the observed frequency-effect function.

Electrical stimulation frequency-effect curves The experimental frequency-effect curves (Figure 2, Table 1) were adequately fitted by a logistic function,

$$E = \frac{a f^n}{f_{50}^n + f^n} \quad , \qquad (1)$$

where a is the maximal asymptote of the frequency-effect curve, f_{50} is the frequency value for $0.5\,a$ and n is the slope parameter. The value of n was found to be 2.28, indicating that the frequency-effect function is 'steep' compared with a rectangular hyperbola (for which $n = 1$).

Acetylcholine concentration-effect curves Logistic curve fitting of the experimental acetylcholine concentration-effect data showed that, at least for exogenously-applied acetylcholine, the relationship was rectangular hyperbolic (Figure 2, Table 1). Therefore it can be written,

$$E = \frac{E_M [A]}{[A_{50}] + [A]} \quad , \qquad (2)$$

where E_M is the maximum acetylcholine-inducible effect and $[A_{50}]$ the value of [A] for $0.5\,E_M$. So long as acetylcholine released *in situ* by electrical stimulation maintains a steady-state, it is reasonable to assume that equation (2), which describes the effects of exogenous acetylcholine, also applies to endogenously-released acetylcholine. The observation that the acid secretion responses, however stimulated, attained a steady-state (Figure 1), although not proof of, is consistent with this assumption.

Electrical stimulation frequency-acetylcholine relation Knowing the form of the frequency-effect and acetylcholine-effect functions (equations (1) and (2), respectively) allows the frequency-acetylcholine relation to be deduced, as follows:

equating (1) and (2) to eliminate E and rearranging gives:

$$[A] = \frac{a [A_{50}] f^n}{E_M f_{50}^n + (E_M - \alpha) f^n} \quad , \qquad (3)$$

which is in the form of the general equation for a logistic function and so is equivalent in form to equation (1). Therefore the frequency-acetylcholine function may be written,

$$[A] = \frac{[A_M] f^n}{K_f^n + f^n} \quad , \qquad (4)$$

where $[A_M]$ is the maximum [A] that electrical stimulation can produce, and K_f is the frequency value for $0.5\,[A_M]$.

Characterization of the electrical stimulation frequency-effect function Having established the form of the input (frequency-acetylcholine) and transducer (acetylcholine-effect) functions the output (frequency-effect) function can be defined by substituting equation (4) in (2) as follows:

$$E = \frac{E_M [A_M] f^n}{K_f^n [A_{50}] + ([A_M] + [A_{50}]) f^n} \qquad (5)$$

The ratio, $[A_M]$:$[A_{50}]$, is analogous to the transducer ratio, τ, which governs the efficacy of one agonist in a system, as previously defined (Black & Leff, 1983). Here, the efficacy of electrical stimulation (frequency) is operationally dependent on the combination of the maximum concentration of released acetylcholine and the potency of acetylcholine. The definition $\tau = [A_M]/[A_{50}]$, expresses this.

Substitution of this definition of τ into equation (5) gives the frequency-effect function in terms of the parameters, τ, E_M, K_f and n, as follows:

$$E = \frac{E_M \tau f^n}{K_f^n + (1 + \tau) f^n} \qquad (6)$$

The model is identical in form to the one previously developed (Black *et al.*, 1985) describing the competitive antagonism of histamine assumed to be released when pentagastrin stimulates gastric acid secretion in the mouse isolated stomach. The only difference is that the pentagastrin-histamine function was 'flat', that is, $n < 1$ in the logistic input function, whereas in the present study the frequency-acetylcholine function has been deduced to be steep ($n > 1$). The reader is referred to the original paper for details of the effects of varying the model parameters.

Competitive antagonism of acetylcholine Competitive antagonism is predicted to affect the location

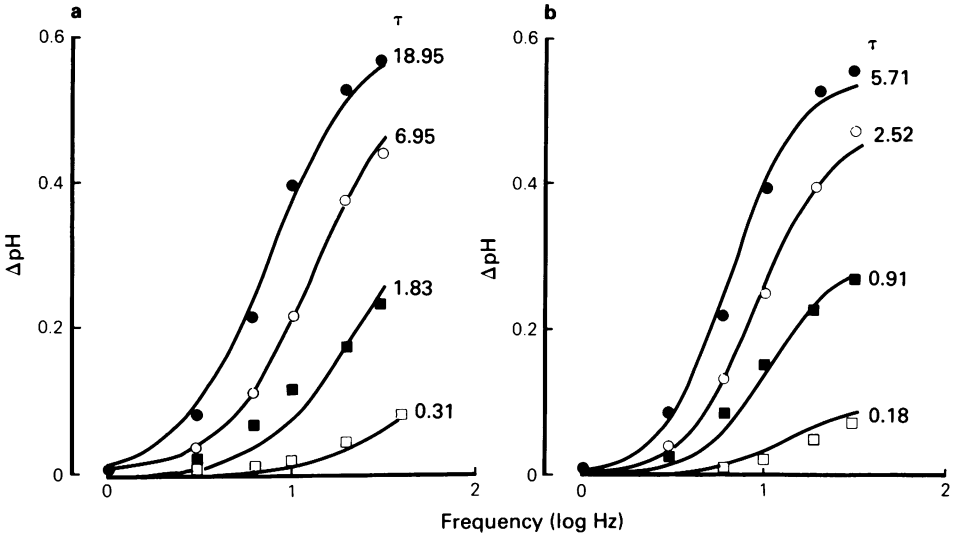

Figure 4 Model fitting of experimental data: the effect of atropine (a) and pirenzepine (b) on frequency-effect curves. The experimental data shown in Figure 2 have been fitted to model equation (6) with E_M constrained to 0.65. The lines drawn through the data are simulations using the parameter values obtained by the model fitting. These parameter values were as follows: atropine (a): n = 1.75, K_f = 42: pirenzepine (b): n = 2.35, K_f = 15.

parameter of the acetylcholine-effect relation in the usual way:

$$\text{dose-ratio} = \frac{[A_{50}]'}{[A_{50}]} = 1 + [B]/K_B \ , \qquad (7)$$

where [B] is the concentration of competitor and K_B its equilibrium dissociation constant; $[A_{50}]'$ is the value of $[A_{50}]$ in the presence of B.

Therefore, assuming that B does not affect the value of $[A_M]$ the ratio of τ values in the presence and absence of B, $\tau':\tau$, equates to the dose-ratio as follows.

$$\frac{\tau}{\tau'} = \frac{[A_M]}{[A_{50}]} \cdot \frac{[A_{50}]'}{[A_M]} = \frac{[A_{50}]'}{[A_{50}]} \qquad (8)$$

Thus, competitive antagonism is predicted to change the value of τ by the factor $(1 + [B]/K_B)$. Substitution of equation (8) into equation (7) provides an equation relating [B] and K_B to τ in the form of a Schild equation,

$$\frac{\tau}{\tau'} - 1 = [B]/K_B \qquad (9)$$

Model fitting of experimental data

The data shown in Figure 3, which illustrates the effect of pirenzepine and atropine on frequency-effect curves, have been simultaneously fitted to equation (6). Due to the nature of the data, that is, depression of the maxima of the curves with only a small degree of rightward shift, convergence could only be achieved when the parameter E_M was given a fixed value of 0.65. This value was the maximum response obtained experimentally with exogenously-applied acetylcholine (Figure 2, Table 1). The fit provided estimates of K_f and n and separate estimates of τ at each concentration of antagonist. The parameter values obtained from the fitting procedure were used to simulate the curves shown superimposed upon the experimental data in Figure 4.

Figure 5 shows the Schild plots previously obtained for the antagonism of 5-methylfurmethide plus 10^{-4} M tiotidine (Black & Shankley, 1985b) and McN-A343 (Black & Shankley, 1985c) by both atropine and pirenzepine, respectively, in the mouse stomach and guinea-pig trachea assays. Also in the figure are the τ values obtained from the model-fitting procedure which have been manipulated according to equation (9). The coincidence of the data obtained on the mouse stomach assay indicates that the changes in τ for frequency-effect curves with the muscarinic antagonists express the apparent affinity of the antagonist in a quantitatively accurate way.

Discussion

Present methods of hormone receptor classification rely on the quantitative use of competitive receptor

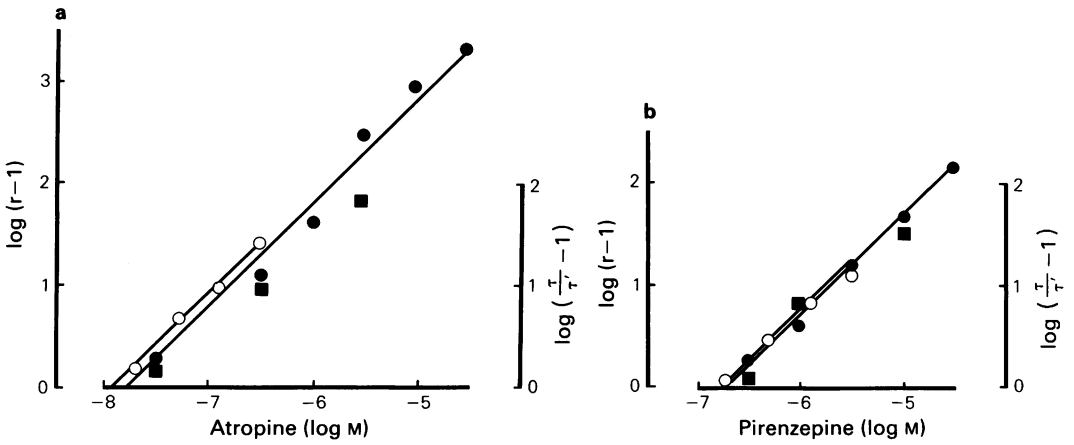

Figure 5 Schild plot representations of the antagonism by atropine (a) and pirenzepine (b) of gastric acid secretion stimulated by 5-methylfurmethide (+ 10^{-4} M tiotidine) (●) and McN-A343 (○) on the mouse stomach assay (data from Black & Shankley, 1985b, c). Shown in addition, are the τ values obtained in this study from the analysis of the antagonism of vagal stimulation (■). These values have been transformed according to equation (9). r = dose-ratio.

antagonists. Simple receptor theory predicts that the reaction between a particular receptor and a competitive antagonist can be characterized by a single parameter, the equilibrium dissociation constant (K_B). This constant provides an unambiguous technique for identifying the receptor with which the antagonist interacts (Arunlakshana & Schild, 1959).

A pK_B value of approximately 8.2 (Brown *et al.*, 1980, North *et al.*, 1985) was found for pirenzepine at M_1-muscarinic receptors and a value of approximately 6.8 at M_2-muscarinic receptors (Szelenyi, 1982; Clague *et al.*, 1985). Thus, the assignment of a particular receptor subtype to the muscarinic receptors involved in neurally-evoked acid secretion requires the demonstration of one of the above values for the K_B for pirenzepine.

In the original studies (Pagani *et al.*, 1984; Schiavone *et al.*, 1985) IC_{50} values were determined for the inhibition of single responses to bethanechol and vagal-stimulated gastric acid secretion by atropine and pirenzepine. Comparison of the ratios of IC_{50} values obtained indicated that pirenzepine demonstrated some selectivity for the inhibition of vagal secretion.

In this study the ability to obtain fully-defined frequency-effect curves, and the subsequent calculation of their operating parameters (Table 1), allowed the development and application of the mathematical model. The model allowed the inhibitory profile observed with the antagonists to be expressed in terms of receptor occupancy and, therefore, an indication of antagonist affinity. In the model the frequency-acetylcholine relation was deduced to be described by a logistic function. In the absence of additional information about the relation between electrical stimulation and acetylcholine, it is perhaps worth noting that there is no physiological information in this finding. The choice of different units of stimulation may well have prompted the application of a different function.

However, the model which was developed appears to provide an adequate description of the experimental results, judged by the reasonable goodness-of-fit obtained with the model-fitting procedure (Figure 4). Atropine and pirenzepine appear to be acting in accordance with the behaviour predicted by the model for simple competitive antagonism at the muscarinic receptor presumed to be involved in the vagal stimulation of gastric acid secretion (Figure 5). Furthermore, the data shown in Figure 5 indicate that pirenzepine and atropine appear to express the same affinity when inhibiting vagal-stimulated gastric acid secretion as they do when inhibiting acid secretion stimulated by 5-methylfurmethide plus 10^{-4} M tiotidine ($pK_B = 6.87 \pm 0.09$: Black & Shankley, 1985b) or McN-A343 ($pK_B = 6.69 \pm 0.07$: Black & Shankley, 1985c). Application of the model allows interpretation of the experimental data without the need to invoke muscarinic heterogeneity. Therefore, we conclude that the results are consistent with the hypothesis that vagal stimulation of gastric acid secretion in the mouse is mediated by acetylcholine which stimulates M_2-muscarinic receptors, which are homogeneous with those found on oxyntic cells. The alternative explanation we previously (Black & Shankley, 1985c) offered for the relatively selective inhibition by pirenzepine of acid secretion, *in vivo*, compared to atropine, is still tenable: atropine, due to high lipophilicity, is lost from the

receptor compartment through the gastric secretion causing apparent underestimation of its affinity relative to pirenzepine.

This work was supported by the Wellcome Foundation Ltd. The authors wish to thank Mrs H.D. Williams for help in preparing the manuscript.

References

ANGUS, J.A. & BLACK, J.W. (1979). Analysis of anomalous pK_B values for metiamide and atropine in the isolated stomach of the mouse. *Br. J. Pharmac.*, **67**, 59–65.

ANGUS, J.A. & BLACK, J.W. (1982). The interaction of choline esters, vagal stimulation and H_2-receptor blockade on acid secretion *in vitro*. *Eur. J. Pharmac.*, **80**, 217–224.

ARUNLAKSHANA, O. & SCHILD, H.O. (1959). Some quantitative uses of drug antagonists. *Br. J. Pharmac.*, **14**, 48–58.

BLACK, J.W. & LEFF, P. (1983). Operational models of agonism. *Proc. R. Soc. Lond. B.*, **220**, 141–162.

BLACK, J.W., LEFF, P. & SHANKLEY, N.P. (1985). Pharmacological analysis of the pentagastrin-tiotidine interaction in the mouse isolated stomach. *Br. J. Pharmac.*, **86**, 589–599.

BLACK, J.W. & SHANKLEY, N.P. (1985a). The isolated stomach preparation of the mouse: a physiological unit for pharmacological analysis. *Br. J. Pharmac.*, **86**, 571–579.

BLACK, J.W. & SHANKLEY, N.P. (1985b). Pharmacological analysis of muscarinic receptors coupled to oxyntic cell secretion in the mouse stomach. *Br. J. Pharmac.*, **86**, 601–607.

BLACK, J.W. & SHANKLEY, N.P. (1985c). Pharmacological analysis of the muscarinic receptors involved when McN-A343 stimulates acid secretion in the isolated mouse stomach. *Br. J. Pharmac.*, **86**, 609–617.

BLACK, J.W. & SHANKLEY, N.P. (1985d). Pharmacological analysis of the inhibition of vagal stimulated acid secretion by pirenzepine and atropine in the isolated mouse stomach. Subtypes of muscarinic receptors: The Second International Symposium. Boston, USA, August 22–24. *Trends Pharmac. Sci.*, suppl. (in press).

BROWN, D.A., FORWARD, A. & MARSH, S. (1980). Antagonist discrimination between ganglionic and ileal muscarinic receptors. *Br. J. Pharmac.*, **71**, 362–364.

CLAGUE, R.U., EGLEN, R.M., STRACHAN, A.C. & WHITING, R.L. (1985). Action of agonists and antagonists at muscarinic receptors present on ileum and atria *in vitro*. *Br. J. Pharmac.*, **86**, 163–170.

DIXON, W.J. (1981). *BMDP Statistical Software*. ed. Dixon, W.J. Berkeley, Los Angeles, London: University of California Press.

NORTH, R.A., SLACK, B.E. & SURPRENAT, A. (1985). Muscarinic M_1 and M_2 receptors mediate depolarization and presynaptic inhibition in guinea pig enteric nervous system. *J. Physiol.*, **368**, 435–452.

PAGANI, F., SCHIAVONE, A., MONFERINI, E., HAMMER, R. & GIACHETTI, A. (1984). Distinct muscarinic receptor subtypes (M_1 and M_2) controlling acid secretion in rodents in: Subtypes of muscarinic receptors. *Trends Pharmac. Sci.*, suppl., 66–68.

SCHIAVONE, A., ANGELICI, O., MICHELETTI, R. & GIACHETTI, A. (1985). M_1 muscarinic antagonists selectively inhibit vagally-induced acid secretion. *Br. J. Pharmac.*, **86**, 798P.

SZELENYI, I. (1982). Does pirenzepine distinguish between 'subtypes' of muscarinic receptors? *Br. J. Pharmac.*, **77**, 567–569.

(Received December 9, 1985.
Revised January 17, 1986.
Accepted January 30, 1986.)